



Velocity field control of robot manipulators by using only position measurements

Javier Moreno-Valenzuela*

*Centro de Investigación y Desarrollo de Tecnología Digital, CITEDI-IPN, Ave. del Parque 1310,
Mesa de Otay, Tijuana, BC 22510, Mexico*

Received 3 September 2005; accepted 17 May 2007

Abstract

In the velocity field control approach the robot motions are specified through a vectorial function that assigns the desired velocity to each point of the configuration space. In other words, a velocity field defines the robot desired velocity in the operational space as a function of its current position. In this paper is introduced a new algorithm to solve the velocity field control formulation in the robot operational space. The proposed approach assumes only joint position measurements and is based on a hierarchical structure that results of using the kinematic control concept and a joint velocity controller. To estimate the joint velocity, nonlinear filtering of the joint position is used.

© 2007 The Franklin Institute. Published by Elsevier Ltd. All rights reserved.

Keywords: Velocity field control; Operational space; Position measurements; Lyapunov function; Stability

1. Introduction

The passive velocity field control introduced in [1,2], attempts to be an alternative to motion control. In this control philosophy, the task to be accomplished by the robot is coded by means of a smooth desired *velocity vector field* defined in the operational configuration space \mathcal{G} and denoted as a map

$$\begin{aligned} \mathbf{v}(\mathbf{y}) : \mathcal{G} &\rightarrow T\mathcal{G} \\ \mathbf{y} &\mapsto \mathbf{v}(\mathbf{y}), \end{aligned}$$

*Tel.: +52 664 623 13 44; fax: +52 664 623 13 88.

E-mail address: moreno@citedi.mx

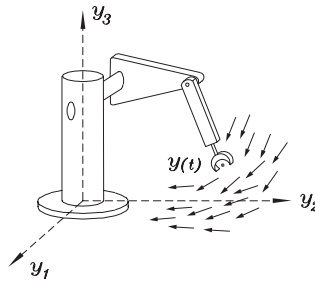


Fig. 1. Desired velocity field in Cartesian space.

where $T_y\mathcal{G}$ is the tangent space of \mathcal{G} at the specific configuration y , and $T\mathcal{G} = \bigcup_{y \in \mathcal{G}} T_y\mathcal{G}$ denotes the tangent bundle of \mathcal{G} [3].

A velocity field defines the desired end-effector velocity at every point of the robot operational configuration space. Fig. 1 illustrates the specification of motion by means of a velocity field. This figure depicts a velocity field defined in the three dimensional Cartesian space of a robot arm which assigns a desired velocity vector (arrow) to each point in the operational space.

The velocity field control is reformulated in this paper without regard of closed-loop passivity requirements [4]:

The velocity field control objective in operational space is established as the design of the torques input τ so that

$$\lim_{t \rightarrow \infty} [v(y(t)) - \dot{y}(t)] = \mathbf{0}, \quad (1)$$

where the difference between the desired velocity field $v(y)$ and the manipulator end-effector velocity \dot{y} defines the velocity field error.

Instead of requiring the arm end-effector tip to be at specific location at each instant time such as it is imposed in trajectory tracking control formulation, in the velocity field control approach the arm tip has to match with the flow lines of the desired velocity field, as it can be seen in Fig. 1. This way of formulating the robot motion is specially important when coordination and synchronization is more important than the time following of a desired trajectory. Velocity field control is well adapted to contour following tasks such as cutting, milling and deburring [5].

The problem of velocity field control in operational space was explored in [4], showing the practical feasibility of two controllers through experimental results in a two degrees-of-freedom direct drive robot. The problem of achieving velocity field control without knowing the robot model has been addressed [6]. There, a proportional-integral controller was analyzed. More recently, the problem of friction compensation when controlling the robot motion along the flow lines produced by a desired velocity field has been discussed in [7].

Practical implementation of control algorithms on robot arms requires velocity measurements, which can be contaminated with noise, especially if tachometers are being used as sensors. This situation together with the discretization of the controller limit the values of the controller gains. As practical solution in the implementation of a controller for mechanical systems, high resolution encoders and hardware that allows high sampling

frequency can be used to approach the velocity measurements via numerical differentiation. However, without high quality hardware one generally finds that numerical differentiation does not work well, especially as the sampling interval decreases, due to the encoder measurement noise [8].

In order to avoid contaminated velocity measurements and simple numerical differentiation of the joint position to estimate the velocity, an approach consists in using the Lyapunov theory to design a controller/filter guaranteeing the robot task execution, no mattering if an estimate of the velocity and acceleration can be possible with the obtained design. This approach increments the robustness with respect to measurement noise and model uncertainties.

The hierarchical control is based on two loops of feedback: A kinematic control loop for joint velocity resolution and an asymptotically stable joint velocity loop. This approach has been exploited in [9] to generate a class of trajectory tracking controllers.

This paper introduces a velocity field controller based on the hierarchical structure of [9] and [10], i.e., a two loops of feedback controller. By using the ideas in [11–13], the proposed solution follows the concept of replacing the joint velocities by the filtering of the joint positions and the desired velocity field via a stable first order filter. Using the Lyapunov theory framework, we present a rigorous stability analysis for the proposed algorithm.

The remaining of this paper is organized as follows. Section 2 deals with the robot dynamics and kinematics. In Section 3, the proposed controller is introduced as well as the discussion on its stability analysis. In Section 4, some remarks on the proposed controller and the stability analysis are presented. Section 5 is devoted to show the simulation results. Finally, some concluding remarks are drawn in Section 6.

Throughout the following notation will be adopted. $\|\mathbf{x}\| = \sqrt{\mathbf{x}^T \mathbf{x}}$ stands for the norm of vector $\mathbf{x} \in \mathbb{R}^n$. $\|B(\mathbf{x})\| = \sqrt{\lambda_M\{B(\mathbf{x})^T B(\mathbf{x})\}}$ stands for the induced norm of a matrix $B(\mathbf{x}) \in \mathbb{R}^{m \times n}$ for all $\mathbf{x} \in \mathbb{R}^n$. $\lambda_{\min}\{A(\mathbf{x})\}$ and $\lambda_{\max}\{A(\mathbf{x})\}$ denote the minimum and maximum eigenvalues of a symmetric positive definite matrix $A(\mathbf{x}) \in \mathbb{R}^{n \times n}$ for all $\mathbf{x} \in \mathbb{R}^n$, respectively.

2. Robot dynamics and kinematics

The dynamics in joint space of a serial-chain n -link robot manipulator considering the presence of friction at the robot joints can be written as [14–16]

$$M(\mathbf{q})\ddot{\mathbf{q}} + C(\mathbf{q}, \dot{\mathbf{q}})\dot{\mathbf{q}} + \mathbf{g}(\mathbf{q}) + F_v \dot{\mathbf{q}} = \boldsymbol{\tau}, \tag{2}$$

where \mathbf{q} is the $n \times 1$ vector of joint displacements, $\dot{\mathbf{q}}$ is the $n \times 1$ vector of joint velocities, $\boldsymbol{\tau}$ is the $n \times 1$ vector of applied torque inputs, $M(\mathbf{q})$ is the $n \times n$ symmetric positive definite manipulator inertia matrix, $C(\mathbf{q}, \dot{\mathbf{q}})\dot{\mathbf{q}}$ is the $n \times 1$ vector of centripetal and Coriolis torques, $\mathbf{g}(\mathbf{q})$ is the $n \times 1$ vector of gravitational torques, and F_v is a $n \times n$ diagonal positive definite matrix which contains the viscous friction coefficients of each joint.

Based on the requirement that matrix $C(\mathbf{q}, \dot{\mathbf{q}})$ is expressed in terms of the Christoffel symbols, the following properties are satisfied.

Property 1. The matrix $C(\mathbf{q}, \dot{\mathbf{q}})$ and the time derivative of the inertia matrix $\dot{M}(\mathbf{q})$ satisfy

$$\mathbf{x}^T [\frac{1}{2} \dot{M}(\mathbf{q}) - C(\mathbf{q}, \dot{\mathbf{q}})] \mathbf{x} = 0 \quad \forall \mathbf{x}, \mathbf{q}, \dot{\mathbf{q}} \in \mathbb{R}^n, \tag{3}$$

$$\dot{M}(\mathbf{q}) = C(\mathbf{q}, \dot{\mathbf{q}}) + C^T(\mathbf{q}, \dot{\mathbf{q}}) \quad \forall \mathbf{q}, \dot{\mathbf{q}} \in \mathbb{R}^n. \quad (4)$$

Property 2. For all $\mathbf{x}, \mathbf{y}, \mathbf{z} \in \mathbb{R}^n$ we have that matrix $C(\mathbf{x}, \mathbf{y})$ satisfies

$$C(\mathbf{x}, \mathbf{y})\mathbf{z} = C(\mathbf{x}, \mathbf{z})\mathbf{y}, \quad (5)$$

$$\|C(\mathbf{x}, \mathbf{y})\mathbf{z}\| \leq k_C \|\mathbf{y}\| \|\mathbf{z}\|, \quad (6)$$

where k_C is strictly positive constant.

Denoting $\mathbf{h}(\mathbf{q}) : \mathbb{R}^n \rightarrow \mathbb{R}^m$ the robot direct kinematics, then the position and orientation $\mathbf{y} \in \mathbb{R}^m$ of the end-effector is given by

$$\mathbf{y} = \mathbf{h}(\mathbf{q}). \quad (7)$$

The time derivative of the direct kinematic model (7) yields the differential kinematic model

$$\dot{\mathbf{y}} = \frac{d}{dt} \mathbf{h}(\mathbf{q}) = \frac{\partial \mathbf{h}}{\partial \mathbf{q}} \dot{\mathbf{q}} = J(\mathbf{q})\dot{\mathbf{q}}, \quad (8)$$

where $J(\mathbf{q})$ is the so-called analytical Jacobian matrix [17]. The robot Jacobian describes a map from velocities in joint space to velocities in operational space. The Jacobian right pseudoinverse [17], is given by

$$J(\mathbf{q})^\dagger = J(\mathbf{q})^T [J(\mathbf{q})J(\mathbf{q})^T]^{-1},$$

assuming that $J(\mathbf{q})J(\mathbf{q})^T$ is nonsingular.

The analytical Jacobian $J(\mathbf{q})$ is assumed of full-rank ($\text{rank} = m$) and bounded by $k_J > 0$, i.e.,

$$\|J(\mathbf{q})\| \leq k_J \quad \forall \mathbf{q} \in \mathbb{R}^n. \quad (9)$$

At the same time, it is also assumed that

$$\|J(\mathbf{q})^\dagger\| \leq k_J^\dagger \quad \forall \mathbf{q} \in \mathbb{R}^n, \quad (10)$$

with $k_J^\dagger > 0$.

The following assumptions on the Jacobian right pseudoinverse time derivative will be useful in the analysis presented in this paper.

Assumption 1. The map expressed by the time derivative of the Jacobian right pseudoinverse satisfies the following relation:

$$\dot{J}(\mathbf{q}, \mathbf{x} + \mathbf{y})^\dagger = \dot{J}(\mathbf{q}, \mathbf{x})^\dagger + \dot{J}(\mathbf{q}, \mathbf{y})^\dagger \quad \forall \mathbf{x}, \mathbf{y} \in \mathbb{R}^n. \quad (11)$$

Assumption 2. The time derivative of the Jacobian right pseudoinverse satisfies the following bound:

$$\left\| \frac{d}{dt} J(\mathbf{q})^\dagger \right\| = \|\dot{J}(\mathbf{q}, \dot{\mathbf{q}})^\dagger\| \leq k_{J1} \|\dot{\mathbf{q}}\|. \quad (12)$$

From a practical point of view, Assumptions 1 and 2 resemble properties more than assumptions.

Some properties of the tangent hyperbolic function will be used. The tangent hyperbolic function is defined as

$$\tanh(x) = \frac{e^x - e^{-x}}{e^x + e^{-x}},$$

and it can be arranged in a vector in the following way:

$$\tanh(\mathbf{z}) = [\tanh(z_1), \dots, \tanh(z_n)]^T$$

and the following properties are accomplished by $\tanh(\mathbf{z})$

(a) The Euclidean norm of $\tanh(\mathbf{z})$ satisfies

$$\|\tanh(\mathbf{z})\| \leq \begin{cases} \|\mathbf{z}\| & \forall \mathbf{z} \in \mathbb{R}^n, \\ \sqrt{n} & \forall \mathbf{z} \in \mathbb{R}^n. \end{cases}$$

(b) The time derivative of $\tanh(\mathbf{z})$ is given by

$$\frac{d}{dt} \tanh(\mathbf{z}) = \text{sech}^2(\mathbf{z}) \dot{\mathbf{z}},$$

where $\text{sech}^2(\mathbf{z}) = \text{diag}\{\text{sech}^2(z_1), \dots, \text{sech}^2(z_n)\}$ and

$$\text{sech}(x) = \frac{2}{e^x + e^{-x}} = \frac{1}{\cosh(x)}.$$

(c) The maximum eigenvalue of the matrix $\text{sech}^2(\mathbf{z})$ is one for all $\mathbf{z} \in \mathbb{R}^n$, i.e.,

$$\lambda_{\text{Max}}\{\text{sech}^2(\mathbf{z})\} = 1 \quad \forall \mathbf{z} \in \mathbb{R}^n.$$

3. A hierarchical approach without velocity measurements

3.1. Velocity field kinematic control

Two important assumptions in the results presented in this paper are

$$\|\mathbf{v}(\mathbf{y})\| \leq v_{M1} \quad \forall \mathbf{y} \in \mathbb{R}^m \tag{13}$$

and

$$\left\| \frac{\partial \mathbf{v}(\mathbf{y})}{\partial \mathbf{y}} \right\| \leq v_{M2} \quad \forall \mathbf{y} \in \mathbb{R}^m. \tag{14}$$

Because the analytical robot Jacobian $J(\mathbf{q})$ is assumed full-rank, and inspired from the resolved motion rate control philosophy [18], we propose the following control law to generate the desired joint velocity ω_d

$$\omega_d(\mathbf{q}) = J(\mathbf{q})^\dagger \mathbf{v}(\mathbf{y}(\mathbf{q})). \tag{15}$$

Note that we have used the notation $\mathbf{y}(\mathbf{q})$ because the posture $\mathbf{y} \in \mathbb{R}^m$ is a function of the joint position $\mathbf{q} \in \mathbb{R}^n$. Inspired in [19], Eq. (15) is called velocity field kinematic control.

Let us define the joint velocity error as

$$\tilde{\omega} = \omega_d(\mathbf{q}) - \dot{\mathbf{q}}. \tag{16}$$

In this way, from the differential kinematic (8) and the definition of the joint velocity error (16) we have

$$\dot{\mathbf{y}} = \mathbf{v}(\mathbf{y}) - J(\mathbf{q})\tilde{\omega}. \tag{17}$$

On the other hand, we can interpret the joint velocity error (16) as the dynamics of the joint position $\mathbf{q} \in \mathbb{R}^n$, i.e.,

$$\dot{\mathbf{q}} = \omega_d(\mathbf{q}) - \tilde{\omega}. \tag{18}$$

Real-time implementation of the kinematic control law (15) requires a joint velocity controller. Then, as soon as the joint velocity error $\tilde{\omega}$ vanishes, the operational space robot velocity $\dot{\mathbf{y}}$ will match the desired velocity field $\mathbf{v}(\mathbf{y})$.

3.2. Joint velocity control

In practice, it is often to find that velocity measurements are corrupted by noise. This situation limits the performance of the robot motions and makes difficult the tuning of the control algorithm. In order to overcome these situations, our key idea is to use a joint velocity controller together with a first order filter to carry out an estimation of the joint velocity. The proposed joint velocity controller is written as follows:

$$\boldsymbol{\tau} = M(\mathbf{q})\dot{\omega}_d^* + C(\mathbf{q}, \omega_d)\omega_d + \mathbf{g}(\mathbf{q}) + K_v \tanh(\dot{\boldsymbol{\xi}}) + F_v \omega_d, \tag{19}$$

$$\dot{\boldsymbol{\xi}} = \omega_d - \boldsymbol{\mathfrak{F}}, \tag{20}$$

where K_v is an $n \times n$ diagonal positive-definite matrix, $\boldsymbol{\mathfrak{F}} \in \mathbb{R}^n$ is the output of a first order filter, the desired joint velocity ω_d is given by (15), and desired joint acceleration ω_d^* is

$$\dot{\omega}_d^* = \dot{J}(\mathbf{q}, \omega_d)^\dagger \mathbf{v}(\mathbf{y}) + J(\mathbf{q})^\dagger \frac{\partial \mathbf{v}(\mathbf{y})}{\partial \mathbf{y}} \mathbf{v}(\mathbf{y}).$$

Fig. 2 shows a general block diagram of the proposed scheme of velocity field control which uses only position measurements as feedback information.

It will be useful to define the function

$$\begin{aligned} \boldsymbol{\eta}(\mathbf{q}, \tilde{\omega}) &= \dot{\omega}_d - \dot{\omega}_d^* \\ &= -\dot{J}(\mathbf{q}, \tilde{\omega})^\dagger \mathbf{v}(\mathbf{y}) + J(\mathbf{q})^\dagger \frac{\partial \mathbf{v}(\mathbf{y})}{\partial \mathbf{y}} J(\mathbf{q})\tilde{\omega}, \end{aligned} \tag{21}$$

which is obtained by using Assumption (11) and Eq. (17). Moreover, it is worthy to observe that $\boldsymbol{\eta}(\mathbf{q}, \tilde{\omega})$ in (21) satisfies the following bound:

$$\begin{aligned} \|\boldsymbol{\eta}(\mathbf{q}, \tilde{\omega})\| &\leq \|\dot{J}(\mathbf{q}, \tilde{\omega})^\dagger \mathbf{v}(\mathbf{y})\| + \|J(\mathbf{q})^\dagger \frac{\partial \mathbf{v}(\mathbf{y})}{\partial \mathbf{y}} J(\mathbf{q})\tilde{\omega}\| \\ &\leq [k_{J1} v_{M1} + k_J^\dagger v_{M2} k_J] \|\tilde{\omega}\| \\ &= k \|\tilde{\omega}\|, \end{aligned} \tag{22}$$

where Assumptions (9)–(11), (13) and (14) were used.

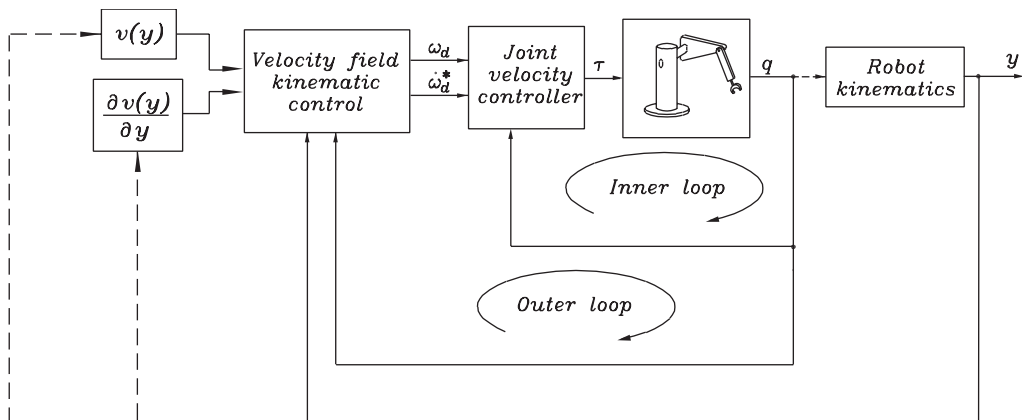


Fig. 2. Block diagram of the velocity field controller which uses only position measurements.

The signal \mathfrak{J} involved in the joint velocity controller (19)–(20) is obtained from the following first order filter

$$\dot{x} = \tanh(\omega_d - \mathfrak{J}) - \omega_d, \tag{23}$$

$$\mathfrak{J} = \omega_d + Ax + Aq, \tag{24}$$

where $A = \text{diag}\{a_1, \dots, a_n\}$ is positive definite.

3.3. Closed-loop system derivation

Differentiating (24) with respect to time, and substituting (23) in the resulting expression, we can write

$$\frac{d}{dt} \mathfrak{J} = \dot{\omega}_d + A \tanh(\omega_d - \mathfrak{J}) - A\omega_d + A\dot{q}. \tag{25}$$

Using the definitions of the joint velocity error $\tilde{\omega}$ in (16) and the signal ξ in (20), it is possible to write (25) as

$$\frac{d}{dt} \xi = -A \tanh(\xi) + A\tilde{\omega}. \tag{26}$$

Eq. (26) resumes the dynamics of the velocity observer (23)–(24).

On the other hand, substituting Eq. (19) in the robot Eq. (2), adding and subtracting $C(q, \dot{q})\omega_d$, and using Assumption (5), we obtain

$$M(q)\dot{\tilde{\omega}} + [C(q, \dot{q}) + C(q, \omega_d)]\tilde{\omega} + K_v \tanh(\xi) + F_v \tilde{\omega} - M(q)\eta(q, \tilde{\omega}) = 0. \tag{27}$$

Eqs. (18), (26) and (27) represent the closed-loop dynamics, that in state variables is given by

$$\Sigma_1: \frac{d}{dt} q = \omega_d(q) - \tilde{\omega}, \tag{28}$$

$$\Sigma_2: \frac{d}{dt} \begin{bmatrix} \xi \\ \tilde{\omega} \end{bmatrix} = \begin{bmatrix} -A \tanh(\xi) + A\tilde{\omega} \\ -M(q)^{-1} \zeta(q, \xi, \tilde{\omega}) + \eta(q, \tilde{\omega}) \end{bmatrix}, \tag{29}$$

where

$$\zeta(\mathbf{q}, \dot{\xi}, \tilde{\omega}) = [C(\mathbf{q}, \omega_d(\mathbf{q}) - \tilde{\omega}) + C(\mathbf{q}, \omega_d(\mathbf{q}))]\tilde{\omega} + K_v \tanh(\dot{\xi}) + F_v \tilde{\omega},$$

$$\omega_d(\mathbf{q}) = J(\mathbf{q})^\dagger \mathbf{y}(\mathbf{q})$$

and $\eta(\mathbf{q}, \tilde{\omega})$ given in (21).

3.4. Stability analysis

In order to consider systems Σ_1 and Σ_2 , as a cascade [20,21], we must prove that the overall system (28)–(29) is complete that is, that the solutions can be continued for all $t \geq 0$ and do not blow up in finite time. This allows us to consider Σ_2 as a time-varying system, that is, we regard the robot-joint velocity controller system as a time-varying system dependent on the joint position $\mathbf{q}(t)$.

3.4.1. Completeness of the closed-loop system

To prove that the system (28)–(29) is complete consider the function

$$W(\mathbf{q}, \dot{\xi}, \tilde{\omega}) = \frac{1}{2} \tilde{\omega}^T M(\mathbf{q}) \tilde{\omega} + \frac{1}{2} \dot{\xi}^T K_v A^{-1} \dot{\xi} + \frac{1}{2} \mathbf{q}^T \mathbf{q},$$

which is a positive definite and radially unbounded function. By virtue of Property 1 in (3), the time derivative of $W(\mathbf{q}, \dot{\xi}, \tilde{\omega})$ along of the closed-loop system trajectories (28)–(29) is given by

$$\begin{aligned} \dot{W}(\mathbf{q}, \dot{\xi}, \tilde{\omega}) = & -\tilde{\omega}^T C(\mathbf{q}, \omega_d(\mathbf{q})) \tilde{\omega} - \tilde{\omega}^T K_v \tanh(\dot{\xi}) \\ & - \tilde{\omega}^T F_v \tilde{\omega} + \tilde{\omega}^T M(\mathbf{q}) \eta(\mathbf{q}, \tilde{\omega}) \\ & - \dot{\xi}^T K_v \tanh(\dot{\xi}) + \dot{\xi}^T K_v \tilde{\omega} + \mathbf{q}^T \omega_d(\mathbf{q}) - \mathbf{q}^T \tilde{\omega}. \end{aligned}$$

It is possible to show that for all $\mathbf{q}, \dot{\xi}, \tilde{\omega} \in \mathbb{R}^n$ the function $\dot{W}(\mathbf{q}, \dot{\xi}, \tilde{\omega})$ attains the inequality

$$\dot{W}(\mathbf{q}, \dot{\xi}, \tilde{\omega}) \leq \kappa_1 W(\mathbf{q}, \dot{\xi}, \tilde{\omega}) + \kappa_2,$$

with κ_1 and κ_2 large enough strictly positive constants. This can be done by invoking the Property 2 in (5) and (6), properties of the tangent hyperbolic function, (10) and (13), and inequality (22).

It follows using the comparison equations method to show that

$$W(t) \leq e^{\kappa_1 t} W(0) + \frac{\kappa_2}{\kappa_1} [e^{\kappa_1 t} - 1],$$

that is, $W(t)$ is bounded for all t bounded and since $W(t)$ is positive definite we obtain that the solutions $[\mathbf{q}(t)^T \ \dot{\xi}(t)^T \ \tilde{\omega}(t)^T]^T$ exist and can be continued for all $t \geq 0$.

3.4.2. Proof of GES

We have proven that the solutions of the closed-loop system Σ_1 – Σ_2 can be continued for all $t \geq 0$ thus the subsystem (29) can be interpret as a nonlinear and nonautonomous system, being the state space origin its unique equilibrium point. In order to show the asymptotic stability of the subsystem Σ_2 in Eq. (29), the following Lyapunov function

candidate is proposed:

$$V(t, \tilde{\omega}, \dot{\xi}) = \frac{1}{2} \tilde{\omega}^T M(\mathbf{q}) \tilde{\omega} + \sum_{i=1}^n k_{vi} a_i^{-1} \ln(|\cosh(\dot{\xi}_i)|) - \alpha \tanh(\dot{\xi})^T M(\mathbf{q}) \tilde{\omega}, \tag{30}$$

where α is a strictly positive constant. With the aim of showing that $V(t, \tilde{\omega}, \dot{\xi})$ is globally positive definite, a lower bound can be computed on $V(t, \tilde{\omega}, \dot{\xi})$ as follows:

$$V(t, \tilde{\omega}, \dot{\xi}) \geq \frac{1}{2} \begin{bmatrix} \|\tanh(\dot{\xi})\| \\ \|\tilde{\omega}\| \end{bmatrix} P \begin{bmatrix} \|\tanh(\dot{\xi})\| \\ \|\tilde{\omega}\| \end{bmatrix},$$

with

$$P = \begin{bmatrix} \lambda_{\min}\{K_v A^{-1}\} & -\alpha \lambda_{\max}\{M(\mathbf{q})\} \\ -\alpha \lambda_{\max}\{M(\mathbf{q})\} & \lambda_{\min}\{M(\mathbf{q})\} \end{bmatrix},$$

and the fact that

$$\sum_{i=1}^n k_{vi} a_i^{-1} \ln(|\cosh(\dot{\xi}_i)|) \geq \frac{1}{2} \tanh(\dot{\xi})^T K_v A^{-1} \tanh(\dot{\xi})$$

was used. A sufficient condition to guarantee that $V(t, \tilde{\omega}, \dot{\xi})$ is positive definite is that P is positive definite, which is satisfied with

$$\alpha < \frac{\sqrt{\lambda_{\min}\{K_v\} \lambda_{\min}\{M(\mathbf{q})\}}}{\sqrt{\lambda_{\max}\{A\} \lambda_{\max}\{M(\mathbf{q})\}}}. \tag{31}$$

The time derivative of $V(t, \tilde{\omega}, \dot{\xi})$ along of the closed-loop system trajectories (29) is given by

$$\begin{aligned} \dot{V}(t, \tilde{\omega}, \dot{\xi}) = & -\tilde{\omega}^T C(\mathbf{q}, \omega_d) \tilde{\omega} - \tilde{\omega}^T F_v \tilde{\omega} + \tilde{\omega}^T M(\mathbf{q}) \eta(\mathbf{q}, \tilde{\omega}) \\ & - \tanh(\dot{\xi})^T K_v \tanh(\dot{\xi}) + \alpha \tanh(\dot{\xi})^T C(\mathbf{q}, \omega_d) \tilde{\omega} \\ & + \alpha \tanh(\dot{\xi})^T K_v \tanh(\dot{\xi}) + \alpha \tanh(\dot{\xi})^T F_v \tilde{\omega} \\ & - \alpha \tanh(\dot{\xi})^T M(\mathbf{q}) \eta(\mathbf{q}, \tilde{\omega}) - \alpha \tanh(\dot{\xi})^T C(\mathbf{q}, \dot{\mathbf{q}})^T \tilde{\omega} \\ & + \alpha \tilde{\omega}^T M(\mathbf{q}) \operatorname{sech}^2(\dot{\xi}) A \tanh(\dot{\xi}) - \alpha \tilde{\omega}^T M(\mathbf{q}) \operatorname{sech}^2(\dot{\xi}) A \tilde{\omega}, \end{aligned}$$

where Property 1 in Eqs. (3)–(4), and Property 2 in Eq. (5) were used. By virtue of the same Properties (Eqs. (3)–(6)), and inequality (22), bounds on each term of the Lyapunov function time derivative $\dot{V}(t, \tilde{\omega}, \dot{\xi})$ can be computed:

$$\begin{aligned} -\tilde{\omega}^T C(\mathbf{q}, \omega_d) \tilde{\omega} & \leq k_C \|\omega_d\|_M \|\tilde{\omega}\|^2, \\ -\tilde{\omega}^T F_v \tilde{\omega} & \leq -\lambda_{\min}\{F_v\} \|\tilde{\omega}\|^2, \\ \tilde{\omega}^T M(\mathbf{q}) [\dot{\omega}_d - \dot{\omega}_d^*] & \leq \lambda_{\max}\{M(\mathbf{q})\} k \|\tilde{\omega}\|^2, \\ -\tanh(\dot{\xi})^T K_v \tanh(\dot{\xi}) & \leq -\lambda_m\{K_v\} \|\tanh(\dot{\xi})\|^2, \\ \alpha \tanh(\dot{\xi})^T C(\mathbf{q}, \omega_d) \tilde{\omega} & \leq \alpha k_C \|\omega_d\|_M \|\tanh(\dot{\xi})\| \|\tilde{\omega}\|, \\ \alpha \tanh(\dot{\xi})^T K_v \tanh(\dot{\xi}) & \leq \alpha \lambda_{\max}\{K_v\} \|\tanh(\dot{\xi})\|^2, \end{aligned}$$

$$\begin{aligned} & \alpha \tanh(\dot{\xi})^T F_v \tilde{\omega} \leq \alpha \lambda_{\text{Max}}\{F_v\} \|\tanh(\dot{\xi})\| \|\tilde{\omega}\|, \\ & -\alpha \tanh(\dot{\xi})^T M(\mathbf{q})[\dot{\omega}_d - \dot{\omega}_d^*] \leq \alpha k \lambda_{\text{Max}}\{M(\mathbf{q})\} \|\tanh(\dot{\xi})\| \|\tilde{\omega}\|, \\ & -\alpha \tanh(\dot{\xi})^T C(\mathbf{q}, \dot{\mathbf{q}})^T \tilde{\omega} \leq \alpha k_C \sqrt{n} \|\tilde{\omega}\|^2 + \alpha k_C \|\omega_d\|_M \|\tanh(\dot{\xi})\| \|\tilde{\omega}\|, \\ & \alpha \tilde{\omega}^T M(\mathbf{q}) \operatorname{sech}^2(\dot{\xi}) A \tanh(\dot{\xi}) \leq \alpha \lambda_{\text{Max}}\{M(\mathbf{q})\} \lambda_{\text{Max}}\{A\} \|\tanh(\dot{\xi})\| \|\tilde{\omega}\|, \\ & -\alpha \tilde{\omega}^T M(\mathbf{q}) \operatorname{sech}^2(\dot{\xi}) A \tilde{\omega} \leq -\alpha \lambda_{\text{min}}\{M(\mathbf{q})\} \lambda_{\text{min}}\{\operatorname{sech}^2(\dot{\xi})\} \lambda_{\text{min}}\{A\} \|\tilde{\omega}\|^2. \end{aligned}$$

An upper bound on $\dot{V}(t, \tilde{\omega}, \dot{\xi})$ can be obtained by using the previous inequalities:

$$\dot{V}(t, \tilde{\omega}, \dot{\xi}) \leq - \begin{bmatrix} \|\dot{\xi}\| \\ \|\tilde{\omega}\| \end{bmatrix}^T Q \begin{bmatrix} \|\dot{\xi}\| \\ \|\tilde{\omega}\| \end{bmatrix} - \phi \|\tilde{\omega}\|^2,$$

where the entries of the matrix Q are

$$\begin{aligned} Q_{11} &= \lambda_{\text{min}}\{K_v\} - \alpha \lambda_{\text{Max}}\{K_v\}, \\ Q_{12} &= -\frac{1}{2}\alpha[\gamma_1 + \lambda_{\text{Max}}\{A\} \lambda_{\text{Max}}\{M(\mathbf{q})\}], \\ Q_{21} &= -\frac{1}{2}\alpha[\gamma_1 + \lambda_{\text{Max}}\{A\} \lambda_{\text{Max}}\{M(\mathbf{q})\}], \\ Q_{22} &= \lambda_{\text{min}}\{F_v\}, \end{aligned}$$

and

$$\phi = \alpha[\lambda_{\text{min}}\{M(\mathbf{q})\} \lambda_{\text{min}}\{\operatorname{sech}^2(\dot{\xi})\} \lambda_{\text{min}}\{A\} - k_C \sqrt{n}] - \gamma_2,$$

with

$$\gamma_1 = 2k_C \|\omega_d\|_M + \lambda_{\text{Max}}\{F_v\} + k \lambda_{\text{Max}}\{M(\mathbf{q})\}, \tag{32}$$

$$\gamma_2 = k_C \|\omega\|_M + k \lambda_{\text{Max}}\{M(\mathbf{q})\}. \tag{33}$$

Sufficient conditions for the matrix Q to be positive definite are

$$\alpha < \frac{\lambda_{\text{min}}\{K_v\}}{2\lambda_{\text{Max}}\{K_v\}}, \tag{34}$$

$$\alpha < \frac{\sqrt{\lambda_{\text{min}}\{K_v\} \lambda_{\text{min}}\{F_v\}}}{\gamma_1 + \lambda_{\text{Max}}\{A\} \lambda_{\text{Max}}\{M(\mathbf{q})\}}, \tag{35}$$

with γ_1 expressed in Eq. (32).

Let us define the set

$$D = \{\dot{\xi} \in \mathbb{R}^n : \|\dot{\xi}\| \leq d\}. \tag{36}$$

Then, for all $\dot{\xi} \in D$ and

$$\lambda_{\text{min}}\{A\} > \frac{k_C \sqrt{n}}{\lambda_{\text{min}}\{M(\mathbf{q})\} \operatorname{sech}^2(d)}, \tag{37}$$

we have that the inequality

$$\alpha > \frac{k_C \|\omega_d\|_M + k \lambda_{\text{Max}}\{M(\mathbf{q})\}}{\lambda_{\text{min}}\{M(\mathbf{q})\} \lambda_{\text{min}}\{A\} \operatorname{sech}^2(d) - k_C \sqrt{n}} \tag{38}$$

guarantees $\phi \geq 0$.

Inequalities (31), (34) and (35) can be satisfied for small enough α , while (38) is satisfied if the product $\lambda_{\text{min}}\{A\} \operatorname{sech}^2(d)$ is sufficiently large. Summarizing, using proper values for

the observer gain A and the control gain K_v we can assure that the inequality

$$\frac{k_C \|\omega_d\|_M + k \lambda_{\text{Max}}\{M(\mathbf{q})\}}{\lambda_{\text{min}}\{M(\mathbf{q})\} \lambda_{\text{min}}\{A\} \text{sech}^2(d) - k_C \sqrt{n}} < \alpha < \min \left\{ \frac{\sqrt{\lambda_{\text{min}}\{K_v\} \lambda_{\text{min}}\{M(\mathbf{q})\}}}{\lambda_{\text{Max}}\{M(\mathbf{q})\} \lambda_{\text{Max}}\{A\}}, \frac{\lambda_{\text{min}}\{K_v\}}{2 \lambda_{\text{min}}\{K_v\}}, \frac{\sqrt{\lambda_{\text{min}}\{K_v\} \lambda_{\text{Max}}\{F_v\}}}{\gamma_1 + \lambda_{\text{Max}}\{A\} \lambda_{\text{Max}}\{M(\mathbf{q})\}} \right\} \quad (39)$$

holds for all $\tilde{\omega} \in \mathbb{R}^n$ and $\dot{\xi} \in D$. A simple tuning procedure to select the gains A and K_v that satisfy the condition (39) is shown in Appendix A. Roughly speaking, the tuning rule consists in using large enough gains A and K_v .

To prove asymptotic stability we invoke similar arguments to the ones used in [22–24]. The Lyapunov function $V(t, \tilde{\omega}, \dot{\xi})$ is globally positive definite and radially unbounded, and its time derivative $\dot{V}(t, \tilde{\omega}, \dot{\xi})$ is negative definite into the set

$$R_A = \{\tilde{\omega} \in \mathbb{R}^n\} \times \{\dot{\xi} \in D\}, \quad (40)$$

where D is described in (36). The domain of attraction contains the largest level set Ω_c of $V(t, \tilde{\omega}, \dot{\xi})$ in R_A , where

$$\Omega_c = \left\{ \begin{bmatrix} \dot{\xi} \\ \tilde{\omega} \end{bmatrix} \in R_A : V(t, \tilde{\omega}, \dot{\xi}) \leq c \right\},$$

and c is a strictly positive constant. Due to the fact that $V(t, \tilde{\omega}, \dot{\xi})$ is globally positive definite and radially unbounded, all level sets Ω_c are contained in R_A , which means that for any initial condition $[\dot{\xi}(0)^T \tilde{\omega}(0)^T]^T \in R_A$ it is always possible to find a constant c such that $[\dot{\xi}(0)^T \tilde{\omega}(0)^T]^T \in \Omega_c$. Therefore, the set $R_A \subset \mathbb{R}^{2n}$ in (40) is forward invariant and all the conditions to prove that the state space origin of the closed-loop system (29) is exponentially stable are satisfied [25]. As result, it is possible to claim that $[\dot{\xi}(t)^T \tilde{\omega}(t)^T]^T \rightarrow 0$ as $t \rightarrow \infty$ for all initial condition $[\dot{\xi}(0)^T \tilde{\omega}(0)^T]^T$ starting at the domain of attraction R_A in (40). The latter together with the assumption that the robot Jacobian is full-rank and bounded allow the conclusion from Eq. (17) that

$$\lim_{t \rightarrow \infty} [\dot{\mathbf{y}}(t) - \mathbf{v}(\mathbf{y}(t))] = \lim_{t \rightarrow \infty} J(\mathbf{q}(t)) \tilde{\omega}(t) = \mathbf{0},$$

which is equivalent to

$$\lim_{t \rightarrow \infty} [\dot{\mathbf{q}}(t) - \omega_d(\mathbf{q}(t))] = \lim_{t \rightarrow \infty} \tilde{\omega}(t) = \mathbf{0}.$$

4. Discussions

- Let us remark that the kinematic control was originally proposed to be used in the joint trajectory tracking control framework and in applications for obstacle avoidance of redundant manipulators. Roughly speaking, the kinematic control problem can be stated as follows: For a given trajectory in the operation space, let us say $\mathbf{y}_d(t)$, find a joint space trajectory $\mathbf{q}_d(t)$ such that $\mathbf{h}(\mathbf{q}_d(t)) = \mathbf{y}_d(t)$. To satisfy this requiring, the kinematic control approach considers that the system input is the joint velocity $\dot{\mathbf{q}}$ and the differential kinematic model (8) is considered as the robot model [15,17,19].
- The real-time implementation of kinematic control requires that the robot at hand is equipped with a joint velocity control system guaranteeing in practice asymptotic

velocity tracking, which corresponds to the controller in Eqs. (19)–(20). This agrees with the actual situation of many industrial robots in that the control of each electro-mechanical axis is carried out using inner joint velocity loops in addition to outer position loops [26,27].

- In practice, the assumption that $J(\mathbf{q})$ is full-rank for all $\mathbf{q} \in \mathbb{R}^n$ cannot be satisfied. Therefore, the controller and the desired velocity field must be constrained to a singularity-free region of the operational space where the Jacobian $J(\mathbf{q})$ is full-rank. When computation of the inverse or pseudoinverse of the Jacobian $J(\mathbf{q})^\dagger$ is required, a damped least-squares inverse can be adopted to improve the robustness in the neighborhood of the kinematic singularities [28].
- The stability result guarantees asymptotic vanishing of the velocity field error for any singularity-free initial configuration $\mathbf{y}(0) \in \mathbb{R}^m$, joint velocity error $\tilde{\omega}(0) \in \mathbb{R}^n$ and $\tilde{\xi}(0) \in D$. Notwithstanding, the assumption of viscous friction at the robot joints allows to invoke the reasoning introduced in [29] to prove the global asymptotic stability of the closed-loop system (29) for a sufficiently small range of desired joint velocity ω_d .
- The attraction domain can be arbitrarily expanded by choosing a large constant d , which enlarges the set D and in consequence the region of attraction R_A . However, increasing of the constant d implies that a large enough numerical value of $\lambda_{\min}\{A\}$ must be specified to satisfy the conditions (37) and (39). In order to achieve this, a tuning procedure is proposed in Appendix A.
- Essentially, the stability result suggests that by using a sufficiently large value of the observer gain A , the control objective is satisfied. At the same time, this implies that we can select K_v so as to avoid actuator saturation and to maintain small amplification of the discretization noise, while the closed-loop system stability is ensured by using high observer gain A .

5. Simulation results

We have carried out numerical simulations using the model of the experimental robot system described in [16]. See Fig. 3 for a scheme of the two degrees-of-freedom robot. The origin of the Cartesian frame is attached at the axis of rotation of the first joint while y_1 and y_2 denote the horizontal and vertical axes, respectively. With this convention, the direct kinematics is given by

$$\mathbf{h}(\mathbf{q}) = \begin{bmatrix} l_1 \sin(q_1) + l_2 \sin(q_1 + q_2) \\ -l_2 \cos(q_1) - l_2 \cos(q_1 + q_2) \end{bmatrix},$$

which leads to the following Jacobian matrix:

$$J(\mathbf{q}) = \begin{bmatrix} l_1 \cos(q_1) + l_2 \cos(q_1 + q_2) & l_2 \cos(q_1 + q_2) \\ l_2 \sin(q_1) + l_2 \sin(q_1 + q_2) & l_2 \sin(q_1 + q_2) \end{bmatrix}.$$

For the robot model $l_1 = l_2 = 0.26$ (m). For self-contents of this paper, the dynamics of the robot arm is described in Appendix B.

The simulation has considered a velocity field that encodes the task of tracing a circle in the operational space. This means that the flow lines of the velocity field converges to

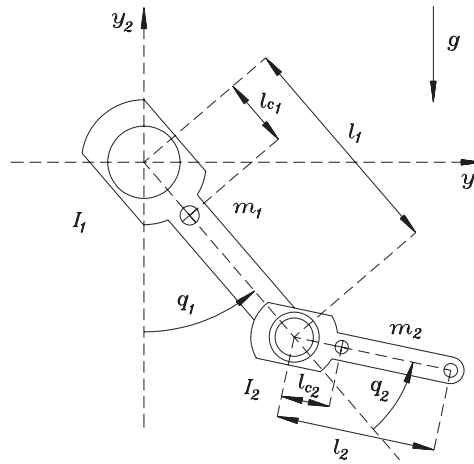


Fig. 3. Scheme of the two degrees-of-freedom robot manipulator.

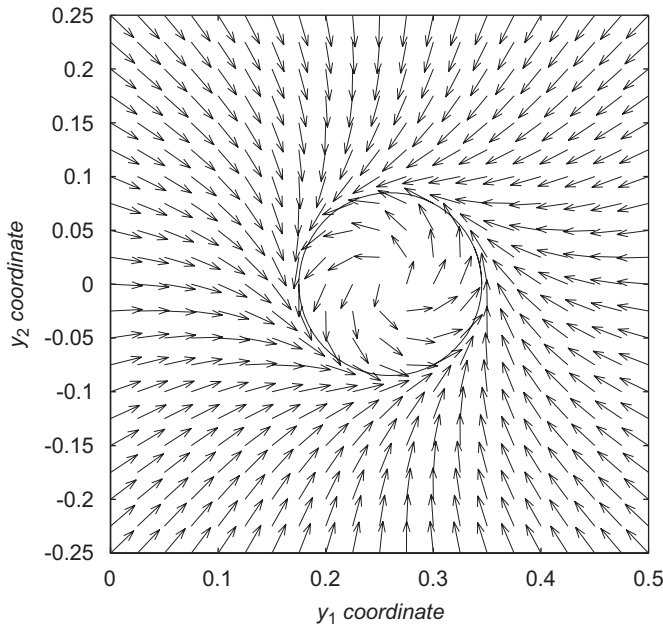


Fig. 4. Desired velocity field used in experiments.

a circular contour. The proposed velocity field $\mathbf{v}(\mathbf{y})$ to generate the flow lines convergent to the circle in the y_1 - y_2 plane is shown in Fig. 4. The desired speed at the circle is $v_0 = 0.65$ (m/s).

The mathematical expression of the desired velocity field $\mathbf{v}(\mathbf{y})$ is given by

$$\mathbf{v}(\mathbf{y}) = -k(\mathbf{y})f(\mathbf{y}) \begin{bmatrix} 2[y_1 - y_{c1}] \\ 2[y_2 - y_{c2}] \end{bmatrix} + c(\mathbf{y}) \begin{bmatrix} -2[y_2 - y_{c2}] \\ 2[y_1 - y_{c1}] \end{bmatrix},$$

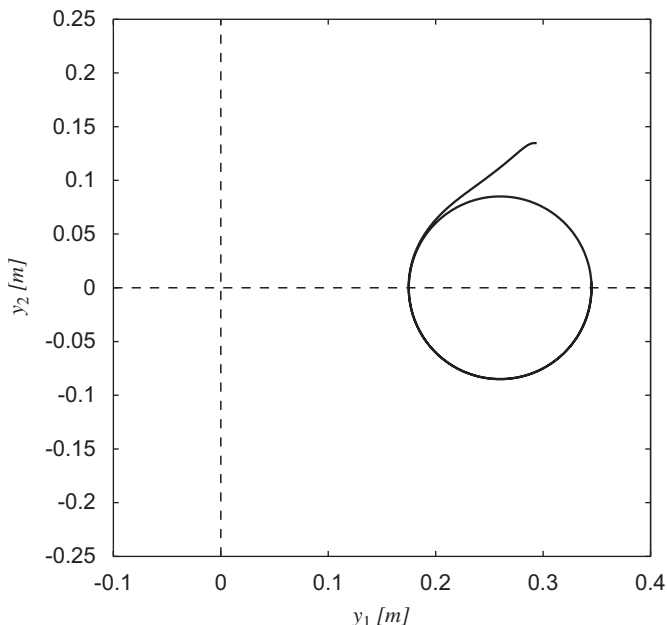


Fig. 5. Robot path in the operational space.

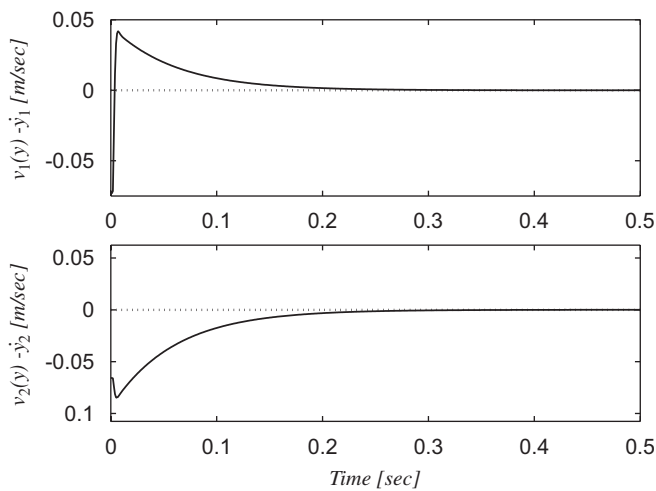


Fig. 6. Velocity field error in operational space.

where $f(\mathbf{y}) = [y_1 - y_{c1}]^2 + [y_2 - y_{c2}]^2 - r_0^2$ with $y_{c1} = 0.26$ (m), $y_{c2} = 0.0$ (m), and $r_0 = 0.085$ (m). Denoting $\nabla f(\mathbf{y})$ the gradient of $f(\mathbf{y})$, the functions $k(\mathbf{y})$ and $c(\mathbf{y})$ are defined as

$$k(\mathbf{y}) = \frac{k_0}{|f(\mathbf{y})| \|\nabla f(\mathbf{y})\| + \varepsilon},$$

$$c(\mathbf{y}) = \frac{v_0 \exp^{-C|f(\mathbf{y})|}}{\|\nabla f(\mathbf{y})\|},$$

where $k_0 = 0.65$ (m/s), $v_0 = 0.65$ (m/s), $C = 50$ (m⁻²), and $\varepsilon = 0.00075$ (m³).

For the velocity field controller (19)–(20), the control gains were

$$K_v = \text{diag}\{5.0, 5.0\} \text{ (1/s)},$$

and in the nonlinear filter (23)–(24) the gain

$$A = \text{diag}\{1000, 1000\} \text{ (1/s)}$$

was used. The results are given in Figs. 5 and 6. They show the Cartesian robot path and the fast convergence of the velocity field error in operational space $\mathbf{v}(\mathbf{y}) - \dot{\mathbf{y}}$.

6. Summary

This paper dealt with the velocity field control of robot arms. The main contribution has been the introduction of a controller which uses only position measurements. This solution consists in a hierarchical control structure based on a kinematic controller for the resolution of the desired joint velocity and an asymptotically stable joint velocity controller. The stability analysis showed the convergence of the operational space velocity $\dot{\mathbf{y}}(t)$ to the desired velocity field $\mathbf{v}(\mathbf{y}(t))$. Simulations were done to assess the practical feasibility of the proposed control law.

Acknowledgment

This work was partially supported by CONACyT Grant 52174 and SIP-IPN Grant 20070202.

Appendix A. Tuning procedure

This Appendix concerns the selection of the gains K_v and A used by the controller (19)–(20) and (23)–(24). From the analysis presented in Section 3.4, it should be noticed that condition (39) synthesizes the way in that the matrices A and K_v can be selected. Namely, the matrix A is involved in the denominator of both sides of the condition (39). The proposed tuning procedure departs from

$$A = \varepsilon_d^2 I_{n \times n} \quad \text{and} \quad K_v = k_v I_{n \times n}. \tag{41}$$

We summarize the three possibilities of condition (39), which were obtained after some direct but tedious algebraic manipulations:

- By using the control gains (41) it is possible to rewrite the inequality

$$\frac{k_C \|\boldsymbol{\omega}_d\|_M + k \lambda_{\text{Max}}\{M(\mathbf{q})\}}{\lambda_{\text{min}}\{M(\mathbf{q})\} \lambda_{\text{min}}\{A\} \text{sech}^2(d) - k_C \sqrt{n}} < \frac{\sqrt{\lambda_{\text{min}}\{K_v\} \lambda_{\text{min}}\{M(\mathbf{q})\}}}{\lambda_{\text{Max}}\{M(\mathbf{q})\} \lambda_{\text{Max}}\{A\}}$$

as a quadratic condition on the gain ε_a

$$\varepsilon_a^2 \underbrace{\lambda_{\min}\{M(\mathbf{q})\} \operatorname{sech}^2(d)}_{C_1} - \varepsilon_a \underbrace{\frac{\lambda_{\max}\{M(\mathbf{q})\}[k_C \|\boldsymbol{\omega}_d\|_M + k \lambda_{\max}\{M(\mathbf{q})\}]}{\sqrt{k_v \lambda_{\min}\{F_v\}}}}_{C_2} - \underbrace{k_C \sqrt{n}}_{C_3} > 0,$$

which is always satisfied with

$$\varepsilon_a > \frac{C_2 + \sqrt{C_2^2 + 4C_1 C_3}}{2C_1}. \tag{42}$$

- Secondly, after substituting the gains (41) into the inequality

$$\frac{k_C \|\boldsymbol{\omega}_d\|_M + k \lambda_{\max}\{M(\mathbf{q})\}}{\lambda_{\min}\{M(\mathbf{q})\} \lambda_{\min}\{A\} \operatorname{sech}^2(d) - k_C \sqrt{n}} < \frac{\lambda_{\min}\{K_v\}}{2 \lambda_{\min}\{K_v\}}$$

we obtain the simple condition

$$\varepsilon_a^2 > \frac{2[k_C \|\boldsymbol{\omega}_d\|_M + k \lambda_{\max}\{M(\mathbf{q})\}] + k_C \sqrt{n}}{\lambda_{\min}\{M(\mathbf{q})\} \operatorname{sech}^2(d)}. \tag{43}$$

- Finally, through the inequality

$$\frac{k_C \|\boldsymbol{\omega}_d\|_M + k \lambda_{\max}\{M(\mathbf{q})\}}{\lambda_{\min}\{M(\mathbf{q})\} \lambda_{\min}\{A\} \operatorname{sech}^2(d) - k_C \sqrt{n}} < \frac{\sqrt{\lambda_{\min}\{K_v\} \lambda_{\max}\{F_v\}}}{\gamma_1 + \lambda_{\max}\{A\} \lambda_{\max}\{M(\mathbf{q})\}}$$

we obtain the tuning rule

$$\varepsilon_a^2 > \left[\frac{\lambda_{\min}\{M(\mathbf{q})\} \operatorname{sech}^2(d)}{k_C \|\boldsymbol{\omega}_d\|_M + k \lambda_{\max}\{M(\mathbf{q})\}} \sqrt{k_v \lambda_{\min}\{F_v\}} - \lambda_{\max}\{M(\mathbf{q})\} \right]^{-1} \\ \times \left[\frac{k_C \sqrt{n} \sqrt{k_v \lambda_{\min}\{F_v\}}}{k_C \|\boldsymbol{\omega}_d\|_M + k \lambda_{\max}\{M(\mathbf{q})\}} - \gamma_1 \right] \tag{44}$$

which is subject to

$$\sqrt{k_v} > \frac{\lambda_{\max}\{M(\mathbf{q})\}[k_C \|\boldsymbol{\omega}_d\|_M + k \lambda_{\max}\{M(\mathbf{q})\}]}{\lambda_{\min}\{M(\mathbf{q})\} \operatorname{sech}^2(d) \sqrt{\lambda_{\min}\{F_v\}}}. \tag{45}$$

The above written inequalities suggest to set the control gain k_v such that the inequality (45) is satisfied and, therefore, to guarantee the existence of the constant α involved in the Lyapunov function $V(t, \tilde{\boldsymbol{\omega}}, \tilde{\boldsymbol{\xi}})$ in (30) is enough to select a large value of observer gain ε_a such that (42), (43) and (44) are attained. In addition, the condition (37) becomes

$$\varepsilon_a^2 > \frac{k_C \sqrt{n}}{\lambda_{\min}\{M(\mathbf{q})\} \operatorname{sech}^2(d)} \tag{46}$$

and it must also be satisfied.

It is noteworthy that the attraction domain can be expanded arbitrarily by choosing a large constant d and ε_a large enough to satisfy (42), (43), (44) and (46).

Appendix B. Robot model

We present below the entries of the robot dynamics described in [16]. The elements $M_{ij}(\mathbf{q})$ ($i, j = 1, 2$) of the inertia matrix are:

$$\begin{aligned} M_{11}(\mathbf{q}) &= 0.3353 + 0.02436 \cos(q_2), \\ M_{12}(\mathbf{q}) &= 0.01267 + 0.01218 \cos(q_2), \\ M_{21}(\mathbf{q}) &= 0.01267 + 0.01218 \cos(q_2), \\ M_{22}(\mathbf{q}) &= 0.01267. \end{aligned}$$

The elements $C_{ij}(\mathbf{q}, \dot{\mathbf{q}})$ ($i, j = 1, 2$) of the centrifugal and Coriolis matrix are

$$\begin{aligned} C_{11}(\mathbf{q}, \dot{\mathbf{q}}) &= -0.01218 \sin(q_2) \dot{q}_2, \\ C_{12}(\mathbf{q}, \dot{\mathbf{q}}) &= -0.01218 \sin(q_2) \dot{q}_1 - 0.01218 \sin(q_2) \dot{q}_2, \\ C_{21}(\mathbf{q}, \dot{\mathbf{q}}) &= 0.01218 \sin(q_2) \dot{q}_1, \\ C_{22}(\mathbf{q}, \dot{\mathbf{q}}) &= 0.0. \end{aligned}$$

The entries of the gravitational torque vector $\mathbf{g}(\mathbf{q})$ are given by:

$$\begin{aligned} g_1(\mathbf{q}) &= g[1.1731 \sin(q_1) + 0.04685 \sin(q_1 + q_2)], \\ g_2(\mathbf{q}) &= g[0.04685 \sin(q_1 + q_2)], \end{aligned}$$

where $g = 9.81$ (m/s²).

The parameters of the viscous friction of the arm are $f_{v_1} = 0.2741$ (Nms/rad) and $f_{v_2} = 0.1713$ (Nm s/rad).

References

- [1] P.Y. Li, R. Horowitz, Passive velocity field control of mechanical manipulators, *IEEE Trans. Robotics Autom.* 15 (4) (1999) 751–763.
- [2] P.Y. Li, R. Horowitz, Passive velocity field control (PVFC): Part I-Geometry and robustness, *IEEE Trans. Autom. Control* 46 (9) (2001) 1346–1359.
- [3] R.M. Murray, Z. Li, S.S. Sastry, *A Mathematical Introduction to Robotic Manipulation*, CRC Press, Boca Raton, FL, 1994.
- [4] J. Moreno, R. Kelly, On manipulator control via velocity fields, in: *Proceedings of the 15th IFAC World Congress, Barcelona, Spain, July, 2002*.
- [5] P.Y. Li, Coordinated contour following control for machining operations—A survey, in: *Proceedings of the American Control Conference, San Diego, CA, June 1999*, pp. 4543–4547.
- [6] I. Cervantes, R. Kelly, J. Alvarez-Ramirez, J. Moreno, A robust velocity field controller, *IEEE Trans. Control Syst. Technol.* 10 (6) (2002) 888–894.
- [7] J. Moreno, R. Kelly, A hierarchical approach to manipulator velocity field control considering dynamic friction compensation, *ASME J. Dyn. Syst. Meas. Control* 128 (3) (2006) 670–674.
- [8] A. Jaritz, M. Spong, An experimental comparison of robust control algorithms on a direct drive manipulator, *IEEE Trans. Control Syst. Technol.* 4 (1996) 627–640.
- [9] R. Kelly, J. Moreno, Manipulator motion control in operational space using joint velocity inner loops, *Automatica* 41 (8) (2005) 1423–1432.
- [10] J. Moreno, R. Kelly, Hierarchical velocity field control, in: *2003 IEEE International Conference on Robotics and Automation, Taipei, Taiwan, September 2003*, pp. 4374–4379.
- [11] A. Loria, R. Ortega, On tracking control of rigid and flexible joint robots, *Appl. Math. Comput. Sci.* 5 (1995) 329–341.
- [12] R. Kelly, A simple set-point robot controller by using only position measurements, in: *Proceedings of the 12th IFAC World Congress, Sydney, Australia, vol. 6, July 1993*, pp. 173–176.

- [13] J. Moreno, R. Kelly, On motor velocity control by using only position measurements: two case studies, *Int. J. Electr. Eng. Educ.* 39 (2) (2002) 118–127.
- [14] M.W. Spong, M. Vidyasagar, *Robot Dynamics and Control*, Wiley, New York, 1989.
- [15] L. Sciavicco, B. Siciliano, *Modeling and Control of Robot Manipulators*, Springer, London, 2000.
- [16] R. Kelly, V. Santibáñez, A. Loria, *Control of Robot Manipulators in Joint Space*, Springer, Berlin, 2005.
- [17] C. Canudas de Wit, B. Siciliano, G. Bastin (Eds.), *Theory of Robot Control*, Springer, London, 1996.
- [18] D.E. Whitney, Resolved motion rate control of manipulators and human prostheses, *IEEE Trans. Man Mach. Syst.* 10 (2) (1969) 47–53.
- [19] B. Siciliano, Kinematic control of redundant robot manipulators, *J. Intelligent Robotic Syst.* 3 (1990) 201–212.
- [20] E. Panteley, A. Loria, On global uniform asymptotic stability of nonlinear time-varying systems in cascade, *Syst. Control Lett.* 33 (1998) 131–138.
- [21] E. Panteley, A. Loria, Growth rate conditions for stability of cascaded time-varying systems, *Automatica* 37 (3) (2001) 453–460.
- [22] E. Zergeroglu, D.M. Dawson, M.S. de Queiroz, M. Krstic, On global output feedback tracking control of robot manipulators, in: *Proceedings of the IEEE Conference on Decision and Control*, Sydney, Australia, December 2000, pp. 5073–5078.
- [23] W.E. Dixon, E. Zergeroglu, D.M. Dawson, Global robust output feedback tracking control of robot manipulators, *Robotica* 22 (4) (2004) 351–357.
- [24] J. Moreno, Design of output feedback tracking controllers for Euler–Lagrange systems by using a Lyapunov function-based procedure, in: *43rd IEEE Conference on Decision and Control*, Atlantis, Paradise Island, Bahamas, December 2004, pp. 4051–4056.
- [25] H. Khalil, *Nonlinear Systems*, Prentice-Hall, Upper Saddle River, NJ, 1996.
- [26] P. Corke, The unimation puma servo system, Report MTM-226, CSIRO Division of Manufacturing Technology, Australia, July, 1994.
- [27] K. Nilsson, *Industrial robot programming*, Ph.D. Thesis, Department of Automatic Control, Lund Institute of Technology, Sweden, 1996.
- [28] C.W. Wampler, L.J. Leifer, Applications of damped least-squares methods to resolved-rate and resolved-acceleration control of manipulators, *ASME J. Dyn. Syst. Meas. Control* 110 (1988) 31–38.
- [29] V. Santibáñez, R. Kelly, Global asymptotic stability of bounded output feedback tracking control for robot manipulators, in: *40th IEEE Conference on Decision and Control*, Orlando, FL, December 2001, pp. 1378–1379.